Chemistry of Metals and Alloys

Chem. Met. Alloys 17 (2024) 45-52
Ivan Franko National University of Lviv
http://publications.lnu.edu.ua/chemetal

Electrochemical synthesis of $Li_{x+y}Tb_5(Sn,Al)_{3-y}$

Vasyl KORDAN[1], Ivan TARASIUK[1]*, Volodymyr PAVLYUK[1]

[1] *Department of Inorganic Chemistry, Ivan Franko National University of Lviv, Kyryla i Mefodiya St. 6, 79005 Lviv, Ukraine*
* *Corresponding author. Tel.:* +380-66-3010259*; e-mail: ivan.tarasiuk@lnu.edu.ua*

Received October 10, 2024; accepted December 17, 2024
https://doi.org/10.30970/cma17.0447

Electrochemical lithiation of the $Tb_5(Sn,Al)_3$ solid solution (Mn_5Si_3-type structure, space group $P6_3/mmc$) was studied by X-ray powder diffraction, scanning electron microscopy, energy-dispersive X-ray spectroscopy, and X-ray fluorescent spectroscopy. It was established that the unit-cell volume of the $Tb_5Sn_{2.5}Al_{0.5}$ and $Tb_5Sn_{2.7}Al_{0.3}$ samples after lithium intercalation increased by 0.5 and 0.9% from 444.70(8) and 445.5(1) Å^3 to 446.9(2) and 449.7(1) Å^3, respectively. For the Li insertion into the crystal structure of the $Tb_5(Sn,Al)_3$ intermetallic, we observed two consecutive processes: I – filling of the octahedral voids with the formation of a structure of the Hf_5CuSn_3-type, and II – partial replacement of tin and aluminum atoms by lithium with the formation of secondary phases such as $Li_{17}Sn_4$ and $LiAl_3$. The amount of electrochemically active lithium was determined; it was 0.42 Li/f.u. (5.3 at.% Li) in the $Tb_5Sn_{2.5}Al_{0.5}$ sample and 0.45 Li/f.u (5.6 at.% Li) in the $Tb_5Sn_{2.7}Al_{0.3}$ sample.

Electrochemical synthesis / Hf_5CuSn_3-type / Li-ion batteries / Mn_5Si_3-type / Solid solution

Introduction

Today, the main trend in scientific research is the synthesis and search for new materials that can accumulate, store and convert electrical energy. Energy-efficient materials attract special attention not only in industry, but also for those who call for a reduction in the use of traditional fuels. It is possible to create multifunctional materials, or significantly improve the characteristics of existing ones, by using chemical tuning. Intermetallic compounds that have a layered crystal structure, lattice defects or large voids, exhibit the ability to intercalate/deintercalate charge carriers, and, therefore, can be used as active materials in batteries. The most important requirements for electrode materials are preservation of the original structure during Li insertion/deinsertion, high sorption capacity, and chemical inertness to electrolyte components [1,2].

Electrochemical processes are influenced by many factors, the most important of which are the structural features and elemental composition of the electrodes. Chemical tuning can reduce the impact of side passivation processes and increase the capacity. The electrochemical lithiation of R_5Sn_3 binary compounds (Mn_5Si_3 structure type, space group $P6_3/mcm$) corresponds to the formation of a Hf_5CuSn_3-type structure and compounds of lithium with tin, for example $Li_{17}Sn_4$ [3-5]. The structural changes and partial substitution of the *p*-element by lithium during electrochemical processes are described in [6-10].

The aim of our investigation was to study the mechanism of lithium insertion into the structure of $Tb_5Sn_{3-x}Al_x$ solid solutions, to carry out phase analysis of the formed products, and to determine the ability of these samples to intercalate/deintercalate lithium reversibly.

Experimental

Mixtures of the pure components, terbium (nominal purity 99.9 wt.%), aluminum (99.99 wt.%), and tin (99.99 wt.%), were melted by arc melting on a water-cooled copper hearth in a purified argon atmosphere using a titanium getter and a tungsten electrode. The alloys were further annealed at 400°C for 2 months in sealed evacuated silica tubes, with quenching into cold water.

The synthesized powder samples were tested as anode material for lithium energy sources. A powder of $LiCoO_2$ ceramic was used as cathode material, whereas an 1M $Li[PF_6]$ solution in 1:1 ethylenecarbonate/dimethylcarbonate acted as electrolyte. The anode and cathode materials were separated by pressed cellulose. A two-electrode

prototype "Swagelok-cell" was used during electrochemical lithiation/delithiation. Electrochemical measurements were carried out in the galvanostatic mode at 0.2 mA/cm^2 using a MTech G410-2 galvanostat [11].

Powder diffraction data were collected on a Proto AXRD Benchtop automatic diffractometer (Cu *K*α-radiation), before and after the electrochemical lithiation. Scanning electron microscopy (SEM) was applied for surface morphology studies. Qualitative and quantitative compositions of the investigated samples before and after the electrochemical processes were determined by energy-dispersive X-ray spectroscopy (EDX) (Tescan Vega3 LMU scanning electron microscope with an Oxford Instruments AZtec ONE System, high vacuum) and X-ray fluorescence spectroscopy (ElvaX Pro X-ray fluorescence analyzer).

Results and discussion

Alloys of the compositions $Tb_5Sn_{2.5}Al_{0.5}$ and $Tb_5Sn_{2.7}Al_{0.3}$ were synthesized for the study. X-ray diffraction and EDX of the samples before measuring their electrochemical characteristics showed that after the homogenization annealing they contained a single phase with a hexagonal structure of the Mn_5Si_3-type (space group $P6_3/mcm$). Fig. 1 (left) shows the surface morphology of the initial sample with the nominal composition $Tb_5Sn_{2.5}Al_{0.5}$. The microcrystallites are irregular in shape and 5-30 μm in size, and have sharp edges. Fig. 1 (right) shows the surface morphology of the sample after lithiation. The surface condition is different, granules and block-like aggregates with a size of 2-20 μm are formed due to adsorption. Fig. 2 presents SEM images of the $Tb_5Sn_{2.7}Al_{0.3}$ sample before and after lithiation. The compositions of the polycrystalline samples $Li_{x+y}Tb_5(Sn,Al)_{3-y}$ from EDX, before and after lithiation, and the corresponding EDX-spectra are presented in Fig. 3.

Elemental mapping of the samples (Fig. 4) shows a uniform distribution and a composition that correlates well with the nominal one. There is a concentration of electrolyte components in aggregates of smaller particles (C, O, F, P). After the electrochemical processes, we observed a slight decrease in the content of tin and aluminum due to side processes. Fig. 5 shows X-ray fluorescence spectra of the initial $Tb_5Sn_{2.5}Al_{0.5}$ sample and the same sample after electrochemical interactions. The Tb/Sn ratio is well correlated with the nominal composition.

The layered nature of the crystal structure of lithium cobaltate facilitates the transfer of lithium from the channels of the structure. Binary compounds of lithium with tin and aluminum are formed during the electrochemical insertion. At the first stage, lithium atoms diffuse into the octahedral voids-channels of the crystal structure of $Tb_5Sn_{3-x}Al_x$. The amount of incorporated lithium corresponds to the limits of the homogeneity range of the resulting phase with the Hf_5CuSn_3 structure type. The homogeneity range of the $Li_xTb_5Sn_3$ and $Li_xTb_5(Sn,Al)_3$ phases synthesized by the thermal synthesis method is about $0 < x < 1$. At the second stage, a decomposition-substitution process takes place, when part of the *p*-element atoms are replaced by lithium atoms. The substituted *p*-element atoms interact with lithium atoms present on the surface of the electrode grains and form the binary intermetallic $Li_{17}Sn_4$ ($Li_{17}Pb_4$-type, space group $F\text{-}43m$) or phases from the Li–Al system. The results of the phase analysis of the solid solutions that served as electrodes are given in Table 1. Fig. 6 shows a projection of the Mn_5Si_3-type crystal structure, which is transformed into a Hf_5CuSn_3-type structure by filling the octahedral voids in Wyckoff position 2*b* with Li atoms.

Table 1 Phase composition of the $Tb_5(Sn,Al)_3$ samples before and after lithiation.

Nominal alloy composition	Phase composition
$Tb_{62.5}Sn_{31.25}Al_{6.25}$ (before lithiation)	**$Tb_5Sn_{2.5}Al_{0.5}$** a = 8.8875(9), c = 6.5010(6) Å, V = 444.70(8) Å^3
$Tb_{62.5}Sn_{31.25}Al_{6.25}$ (after lithiation)	**$Tb_5Sn_{2.5}Al_{0.5}$:*x*Li** a = 8.895(1), c = 6.523(1) Å, V = 446.9(2) Å^3 **$Li_{17}Sn_4$**, **$LiAl_3$**, **Li_3Al_2** – trace amounts
$Tb_{62.5}Sn_{33.75}Al_{3.75}$ (before lithiation)	**$Tb_5Sn_{2.7}Al_{0.3}$** a = 8.889(1), c = 6.511(1) Å, V = 445.5(1) Å^3
$Tb_{62.5}Sn_{33.75}Al_{3.75}$ (after lithiation)	**$Tb_5Sn_{2.7}Al_{0.3}$:*x*Li** a = 8.922(1), c = 6.523(1) Å, V = 449.7(1) Å^3 **$Li_{17}Sn_4$**, **$LiAl_3$**, **Li_3Al_2** – trace amounts
$Tb_{62.5}Sn_{37.5}$ (before lithiation)	**Tb_5Sn_3** [8] a = 8.9075(5), c = 6.5023(4) Å, V = 446.80(5) Å^3
$Tb_{62.5}Sn_{37.5}$ (after lithiation)	**Tb_5Sn_3:*x*Li** [8] a = 8.9229(4), c = 6.5221(4) Å, V = 449.71(4) Å^3 **$Li_{17}Sn_4$** – trace amounts

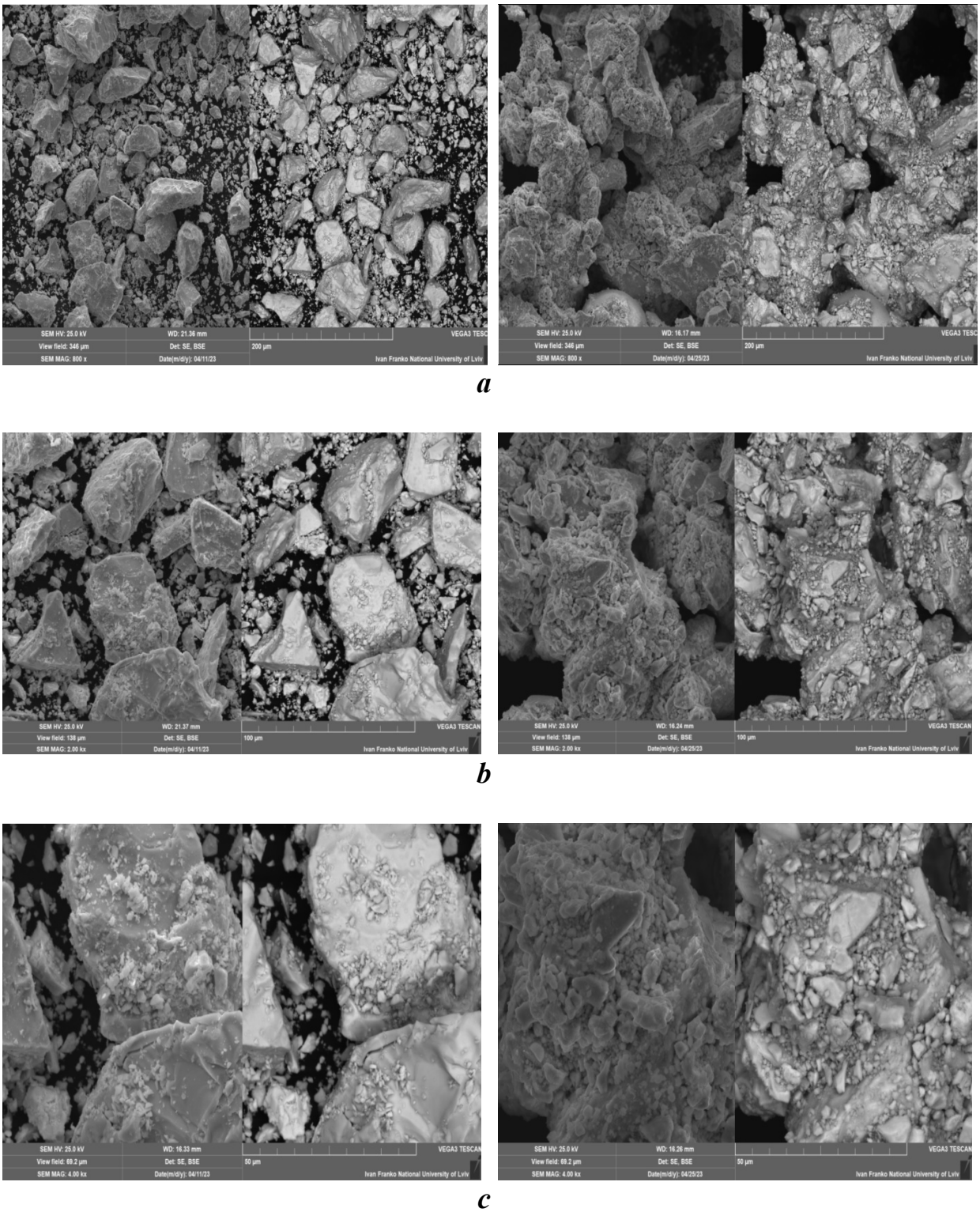

Fig. 1 SEM-images of the $Tb_5Sn_{2.5}Al_{0.5}$ sample before (left) and after (right) lithiation, magnification 800 (*a*), 2000 (*b*) and 4000 (*c*) times.

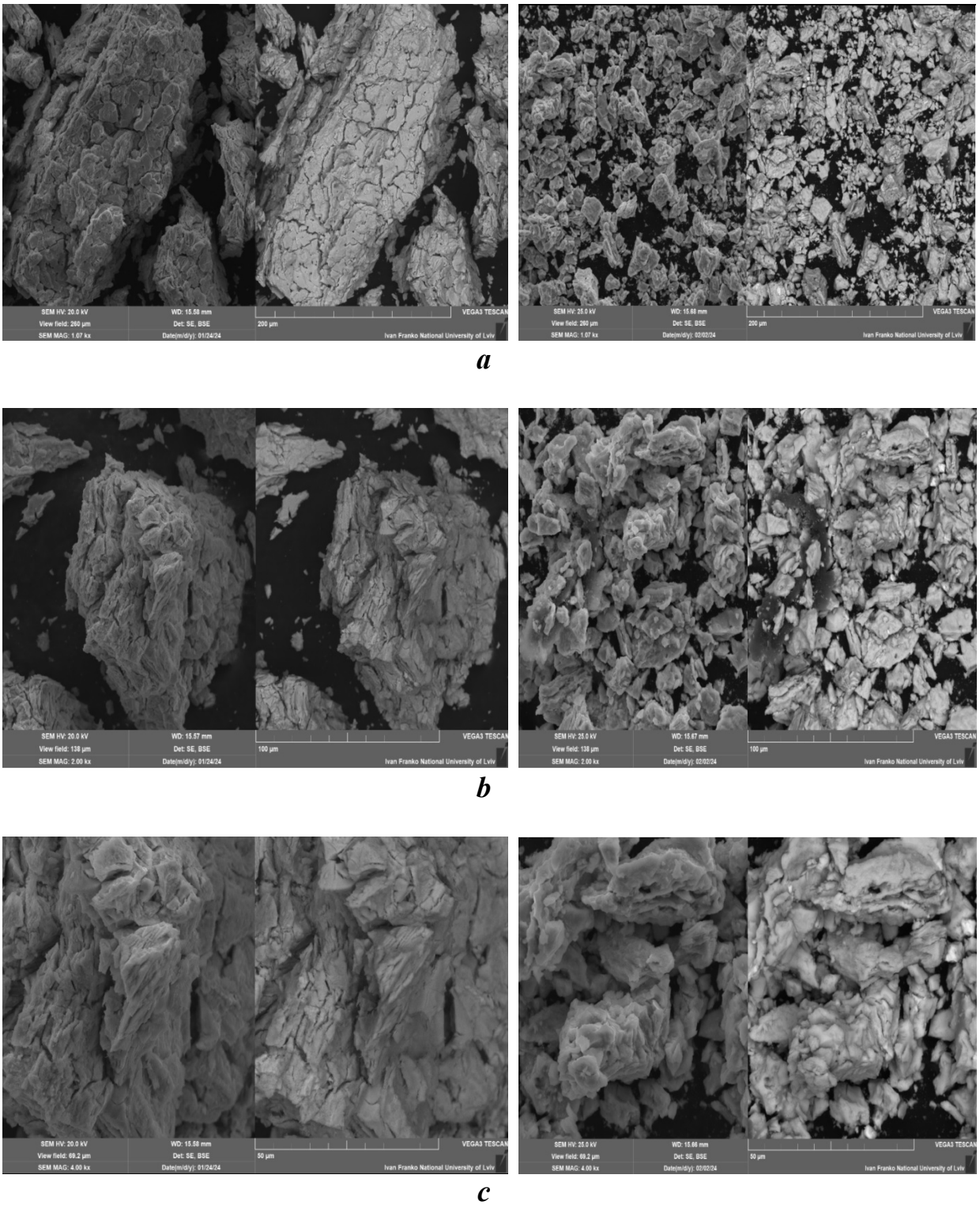

Fig. 2 SEM-images of the $Tb_5Sn_{2.7}Al_{0.3}$ sample before (left) and after (right) lithiation, magnification 1070 (*a*), 2000 (*b*) and 4000 (*c*) times.

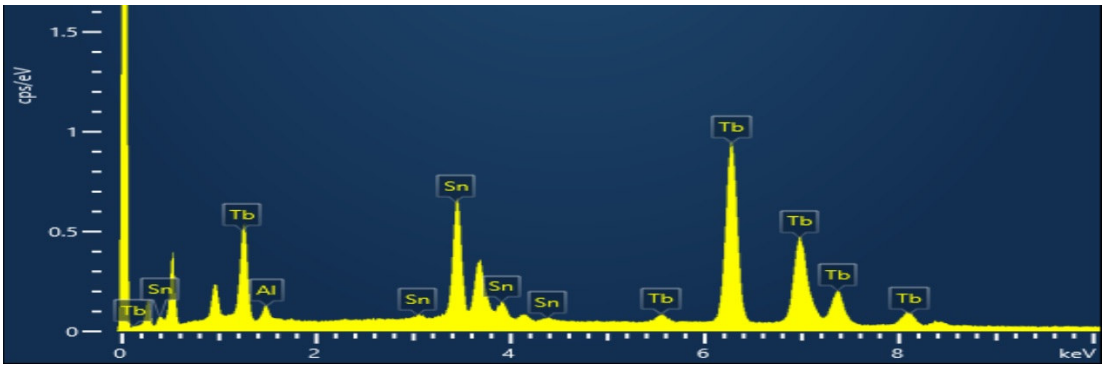

a ($Tb_{62.7}Sn_{30.9}Al_{6.4}$)

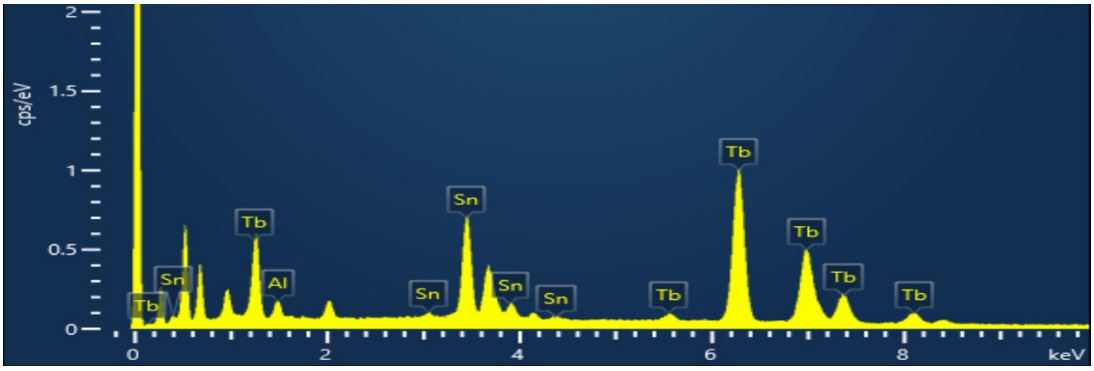

b ($Tb_{63.6}Sn_{30.3}Al_{6.1}$)

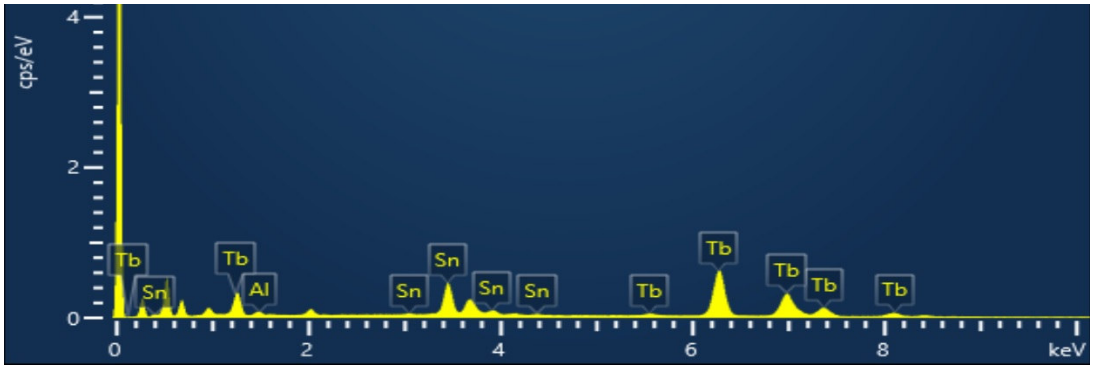

c ($Tb_{62.1}Sn_{34.5}Al_{3.4}$)

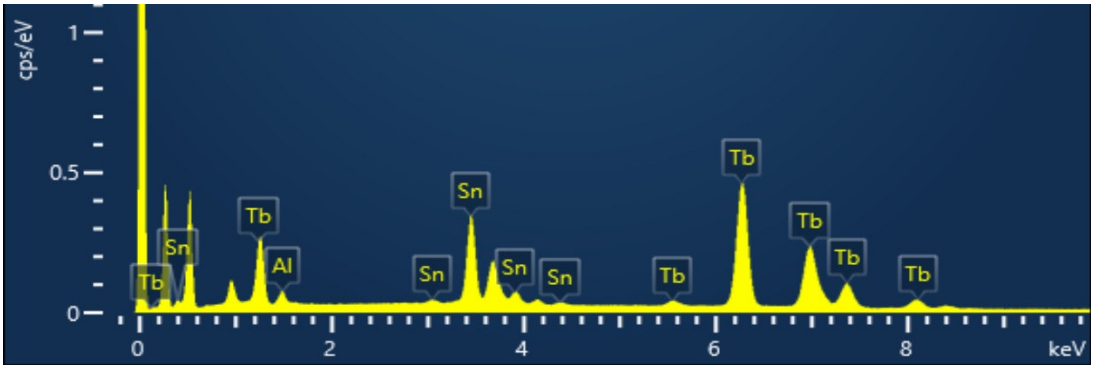

d ($Tb_{64.2}Sn_{33.1}Al_{2.7}$)

Fig. 3 EDX-spectra of the polycrystalline samples $Tb_5Sn_{2.5}Al_{0.5}$ and $Tb_5Sn_{2.7}Al_{0.3}$ before (*a* and *c*) and after (*b* and *d*) lithiation (without C, O, F and P).

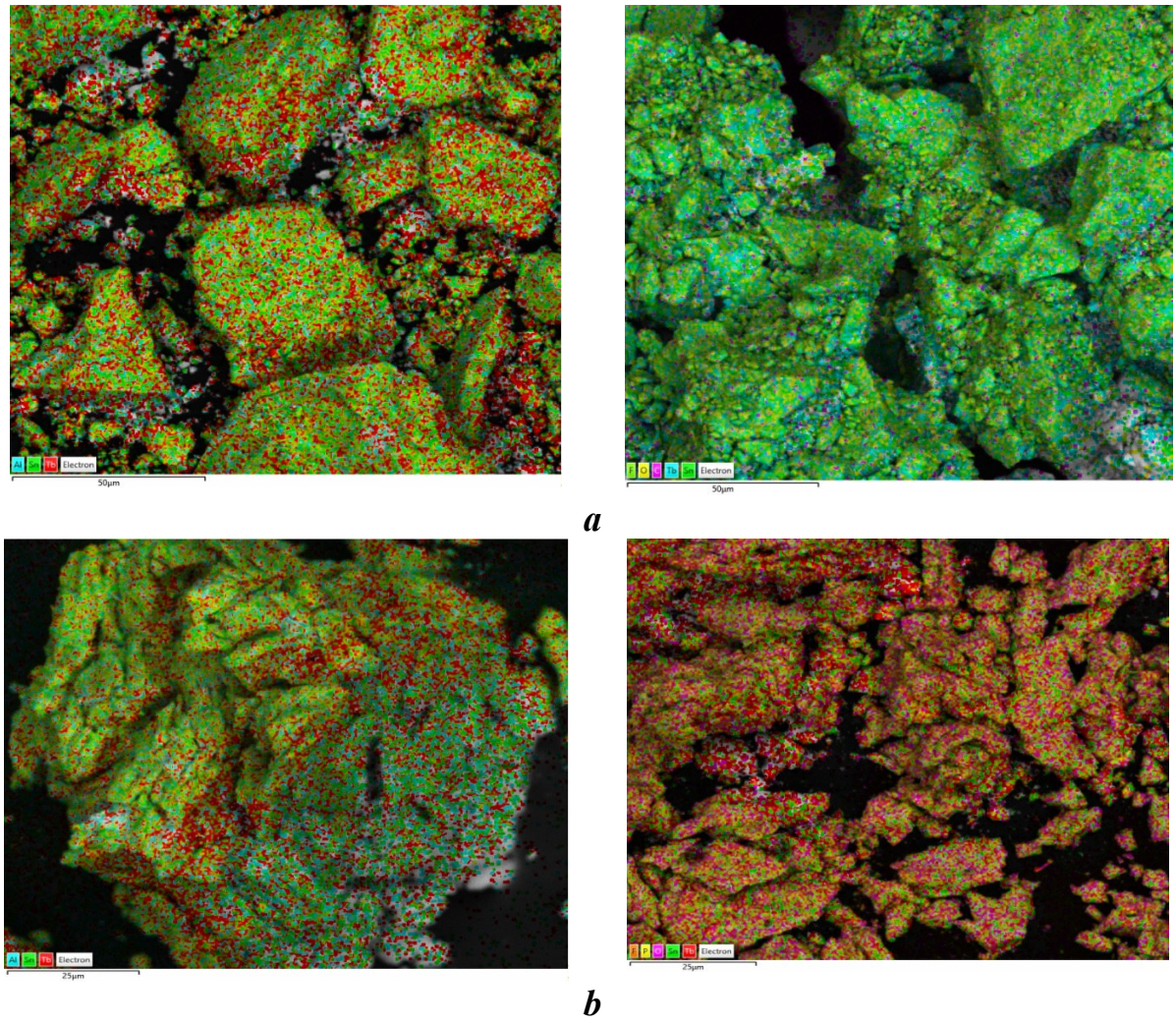

Fig. 4 Elemental mapping of the samples $Tb_5Sn_{2.5}Al_{0.5}$ (*a*) and $Tb_5Sn_{2,7}Al_{0,3}$ (*b*) before (left) and after (right) lithiation.

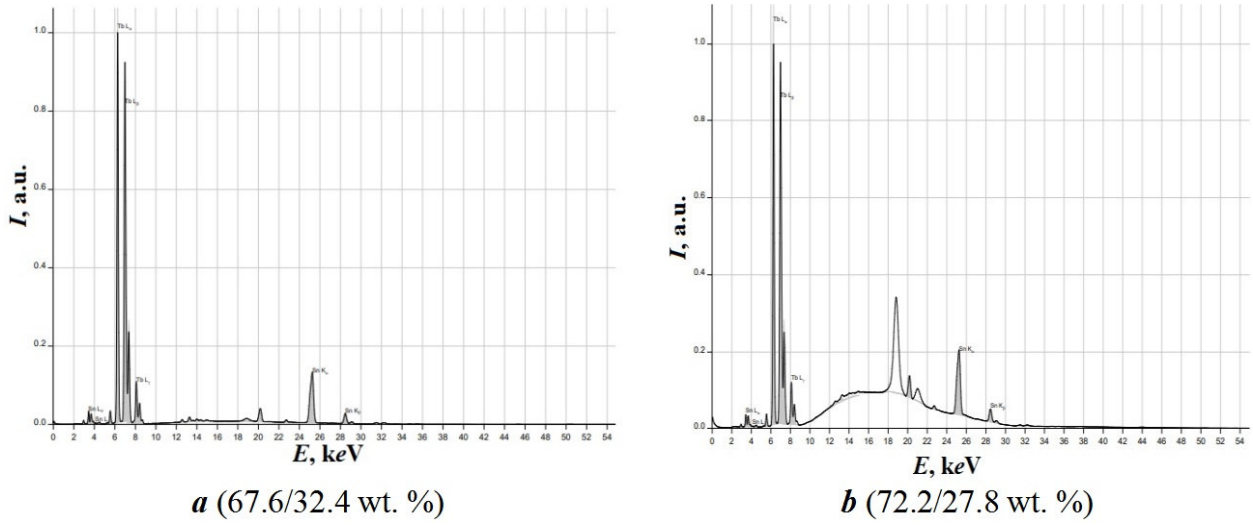

Fig. 5 X-ray fluorescent spectra of $Tb_5Sn_{2.5}Al_{0.5}$ before (*a*) and after (*b*) lithiation.

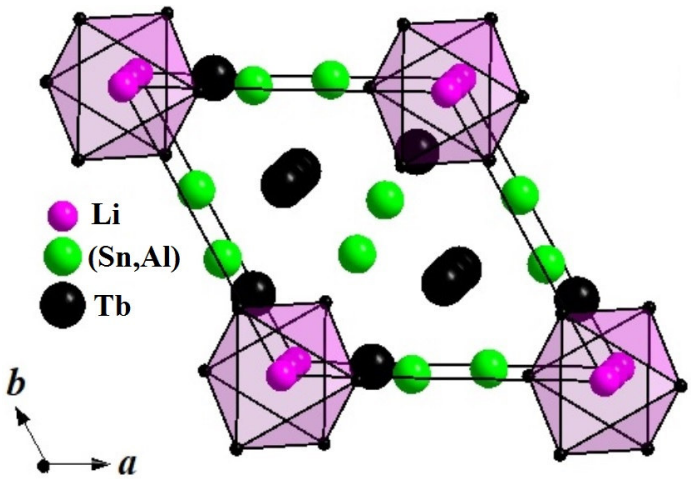

Fig. 6 Unit cell of the solid solution $Li_xTb_5(Sn,Al)_3$ and coordination polyhedra of the Li atoms.

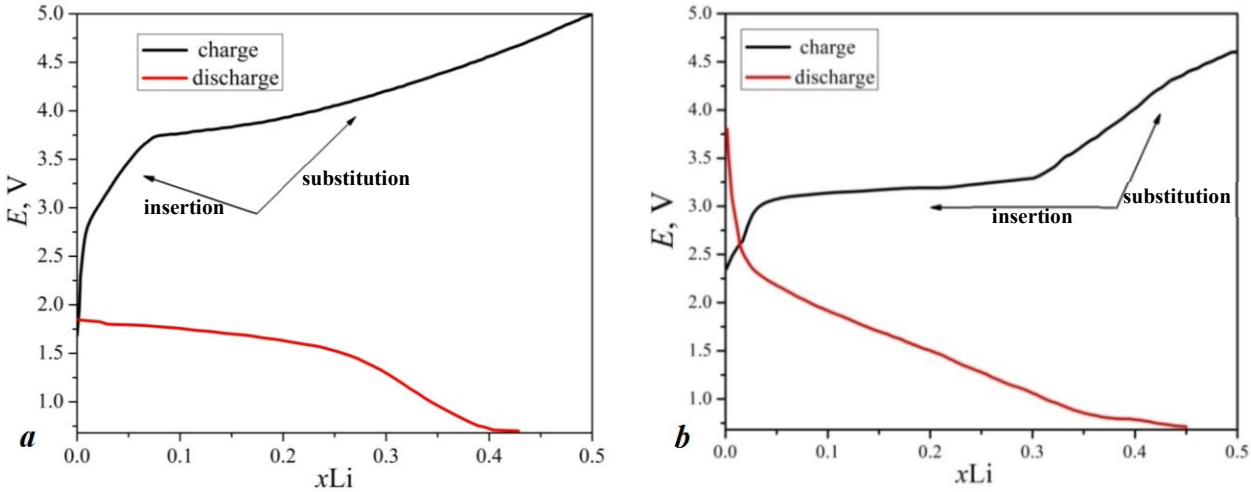

Fig. 7 Selected charge and discharge curves for battery prototypes with electrodes based on $Tb_5Sn_{2.5}Al_{0.5}$ (*a*) and $Tb_5Sn_{2.7}Al_{0.3}$ (*b*).

Intercalating lithium into the structure, we clearly observed two plateaus of electrochemical reactions on the charging curves. The alloys studied as electrode materials partially lost crystallinity due to electrochemical processes. The surface of the alloy grains changed to porous and was aggregated by electrolyte components. The amount of electrochemically active lithium in the structure of $Tb_5Sn_{2.5}Al_{0.5}$ was 0.42 Li/f.u. (5 at.% Li), for the sample with lower aluminum content it was 0.45 Li/f.u. (Fig. 7). The charge-discharge characteristics demonstrate the two-stage nature of the lithiation process and confirm the suggestion regarding the existence of two consecutive electrochemical processes. Li-containing multicomponent compounds in the form of microcrystallites have been deposited on larger grains of the material. In all cases the surface acquired a larger specific area and became looser.

When studying $Tb_5Sn_{2.7}Al_{0.3}$ and $Tb_5Sn_{2.5}Al_{0.5}$ as electrodes (charging process at 1.0 mA/cm^2), it was found that up to 2.8 and 3.7 V, lithium incorporation into 2*b* voids takes place; above this an increase in potential is observed, which has the form of a break, where partial substitution of Li for Sn occurs (Fig. 7*a*). The maximum Li content in the Al-free phases $Li_xTb_5M_3$ (M = Sn or Sb, synthesized by the electrochemical method) is somewhat smaller than the amount of lithium in the same compounds synthesized by the thermal method, since, under the experimental conditions used here it does not exceed ~0.4 Li atoms/f.u. for Tb_5Sn_3 and ~0.2 Li atoms/f.u. for Tb_5Sb_3 [8]. After the electrochemical lithiation, amorphization of the material (reduction of the grain size) was observed. This was confirmed by comparing SEM images of polycrystalline samples of the initial solid solutions with SEM images of powders after lithium insertion.

Electrodes based on the studied samples showed satisfactory results in terms of the amount of intercalated lithium and discharge capacity. During the investigation (up to 50 cycles), we observed loss of capacity of the prototype battery due to side electrochemical processes, such as significant amorphization of the material and passivation by electrolyte components of the surface of the Li-containing phases. The surface of the alloys can interact with electrolyte components and the environment, adsorbing light (water, oxygen) and heavier (electrolyte molecules) molecules. Then it is necessary to tune the conditions (current density and strength, voltage and environment) to electrochemically dissolve the unwanted adsorbed interphase and restore the surface for lithium insertion in the structural voids of the solid phase.

Summary

The process of lithiation of the $Tb_5(Sn,Al)_3$ phase consists of two stages. At the first stage, lithium atoms are inserted into the octahedral voids-channels of the crystal structure. At the second stage, part of the *p*-element atoms are replaced by lithium atoms, and the substituted *p*-element atoms interact with lithium atoms on the surface of the alloy. The composition of the grains after lithiation changed in favor of terbium. Microcrystallites with a size of 200-600 nm (SEM-method) were formed by reducing the grains of the electrodes. Small aggregates (2-20 μm) were formed based on these particles as a result of material amorphization and interaction of the electrode surface with the electrolyte. The cell parameters of the $Tb_5Sn_{2.5}Al_{0.5}$ and $Tb_5Sn_{2.7}Al_{0.3}$ samples increased from a = 8.8875(9), c = 6.5010(6) Å and a = 8.889(1), c = 6.511(1) Å to a = 8.895(1), c = 6.523(1) Å and a = 8.922(1), c = 6.523(1) Å, respectively, after lithium intercalation. The reversible amount of lithium was 0.42 Li/f.u. (5.3 at.% Li) for the electrode based on the $Tb_5Sn_{2.5}Al_{0.5}$ sample and 0.45 Li/f.u. (5.6 at.% Li) for the $Tb_5Sn_{2.7}Al_{0.3}$ alloy.

Acknowledgements

Funding for this research was provided by the Ministry of Science and Education of Ukraine grant "High-capacity power elements and ultra-hard ceramic coatings for civilian and military purposes" (No. 0124U001013) and the grant "Search for new structure types" (HX-010324) of the company Material Phases Data System, Switzerland.

References

[1] C.A. Vincent, B. Scrosati, *Modern Batteries. An Introduction to Electrochemical Power Sources*, 2nd ed., Butterworth-Heinemann, Oxford, 1997, 368 p.
[2] J.O. Besenhard, *Handbook of Battery Materials*, Wiley-VCH, Weinheim, 1999, 618 p.
[3] A. Stetskiv, V. Kordan, I. Tarasiuk, O. Zelinska, V. Pavlyuk, *Chem. Met. Alloys* 7 (2014) 106-111.
[4] A. Balińska, V. Kordan, R. Misztal, V. Pavlyuk, *J. Solid State Electrochem*. 19(8) (2015) 2481-2490.
[5] G. Kowalczyk, V. Kordan, A. Stetskiv, V. Pavlyuk, *Intermetallics* 70 (2016) 53-60.
[6] V. Kordan, O. Zelinska, I. Tarasiuk, R. Serkiz, V. Pavlyuk, *Visn. Lviv. Univ., Ser. Khim*. 59(1) (2018) 115-122.
[7] V. Kordan, O. Zelinska, V. Pavlyuk, I. Oshchapovsky, R. Serkiz, *Chem. Met. Alloys* 9(1/2) (2016) 84-91.
[8] V. Kordan, O. Zelinska, V. Pavlyuk, *Visn. Lviv. Univ., Ser. Khim*. 58(1) (2017) 108-116.
[9] V. Kordan, V. Pavlyuk, O. Zelinska, *Visn. Lviv. Univ., Ser. Khim*. 57(1) (2016) 148-154.
[10] V. Kordan, O. Zhyshkovych, O. Zelinska, I. Tarasiuk, V. Pavlyuk, R. Serkiz, *Visn. Lviv. Univ., Ser. Khim*. 60(1) (2019) 127-139.
[11] MTech [Online source] – Retrieved from: http://mtech-lab.com.ua/index.htm.